

# Lensing Bias in Cosmic Shear

Fabian Schmidt,<sup>1,2</sup> Eduardo Rozo,<sup>3</sup> Scott Dodelson,<sup>4,1,2</sup> Lam Hui,<sup>5,6</sup> and Erin Sheldon<sup>7</sup>

<sup>1</sup>*Department of Astronomy & Astrophysics, The University of Chicago, Chicago, IL 60637*

<sup>2</sup>*Kavli Institute for Cosmological Physics, Chicago, IL 60637*

<sup>3</sup>*CCAPP, The Ohio State University, Columbus, OH 43210*

<sup>4</sup>*Center for Particle Astrophysics, Fermi National Accelerator Laboratory, Batavia, IL 60510*

<sup>5</sup>*Institute for Strings, Cosmology, and Astroparticle Physics (ISCAP)*

<sup>6</sup>*Department of Physics, Columbia University, New York, NY 10027*

<sup>7</sup>*Brookhaven National Laboratory, Upton, NY 11973*

Only galaxies bright enough and large enough to be unambiguously identified and measured are included in galaxy surveys used to estimate cosmic shear. We demonstrate that because gravitational lensing can scatter galaxies across the brightness and size thresholds, cosmic shear experiments suffer from *lensing bias*. We calculate the effect on the shear power spectrum and show that – unless corrected for – it will lead analysts to cosmological parameters estimates that are biased at the  $2 - 3\sigma$  level in DETF Stage III experiments, such as the Dark Energy Survey.

## I. INTRODUCTION

Weak gravitational lensing has emerged as a powerful tool to probe cosmological models. Current measurements [1–3] already constrain the amplitude of density perturbations in the universe and the total matter density. Future surveys are projected to have the power to constrain the most important parameters describing both dark energy [4, 5] and dark matter [6–9].

While the largest uncertainties in these projections are experimental systematics, a lingering concern is our ability to make predictions for basic quantities such as the two-point function to sub-percent accuracy so that theoretical systematics will not be an issue. A number of higher order corrections to the two-point function have been considered: the Born correction, source-lens coupling, reduced shear, and lens-lens coupling [10–12]. Here we study another effect which contaminates the power spectrum at the same level as these [13]: *lensing bias*.

Galaxies are selected in weak lensing surveys only if they are bright enough and large enough for their shapes to be adequately measured. Lensing affects these criteria because galaxies too faint or small to make it into the catalog can be promoted into the sample if they are located in regions of large magnification. This effect is inevitable as it is only possible to cut on *observed* sizes and magnitudes, and cannot be eliminated by imposing brighter magnitude cuts.

To appreciate the importance of this effect, consider a cartoon universe in which all galaxies are just a little too faint to be included in the survey. In this case, only galaxies behind regions of large magnification would be included, so one would be able to estimate shear only behind foreground matter overdensities. The ensuing shear map would be a map of clusters! Of course, reality is much more complicated than this toy example, and many galaxies will be in the survey by their own merits. Moreover, the sky-dilution from lensing will compete with the effect we just described, so whether matter overdensities are over-sampled or under-sampled depends on the galaxy population. Nevertheless, it is clear that the sampling of the cosmic shear field from a typical galaxy survey will almost always be biased. In this paper, we derive this lensing bias and study its effect on the shear power spectrum. We also discuss how it affects other shear observables.

In Section II, we present and discuss the leading lensing bias corrections. Section III then calculates the correction to the shear power spectrum, while other shear observables are discussed in Section IV. We conclude in Section V. The appendices contain a rigorous derivation of the leading and higher order correction terms, and discuss why the higher order terms can be neglected for the purposes of near-future surveys.

## II. LENSING BIAS AND COSMIC SHEAR

This section describes the leading order lensing bias effects on cosmic shear. For a rigorous derivation and treatment of higher order terms, see Appendices A and C. Let us consider a survey of solid angle  $\Delta\Omega$  with  $N_{\text{tot}}$  observed galaxies in total, so that the observed average number density is  $\bar{n} = N_{\text{tot}}/\Delta\Omega$ .

To first order, the *observed* galaxy overdensity  $\delta_{\text{obs}}$  is given in terms of the intrinsic galaxy overdensity  $\delta_g$  and the convergence  $\kappa$  by [14]:

$$\delta_{\text{obs}}(\vec{\theta}) = \delta_g(\vec{\theta}) + q \kappa(\vec{\theta}), \quad (1)$$

where  $q = 2\beta_f + \beta_r - 2$ , and  $\beta_f$  and  $\beta_r$  are the logarithmic slopes of the flux and size distributions,

$$\beta_f = -\left. \frac{\partial \ln n_{\text{obs}}}{\partial \ln f} \right|_{\substack{f=f_{\text{min}} \\ r=r_{\text{min}}}}; \quad \beta_r = -\left. \frac{\partial \ln n_{\text{obs}}}{\partial \ln r} \right|_{\substack{f=f_{\text{min}} \\ r=r_{\text{min}}}}. \quad (2)$$

In the following,  $\delta_{\text{obs}}$  will always stand for the background galaxies whose shear is measured, while foreground galaxy overdensities we correlate with will be denoted with  $\delta_{\text{obs}}^{\text{fg}}$  for clarity.

In the weak lensing limit, cosmic shear can be described by a spin-2 field with two independent components, defined relative to fixed coordinate axes  $x, y$  ( $\rightarrow \gamma_1, \gamma_2$ ), or with respect to the separation vector  $\vec{\theta}$  ( $\rightarrow \gamma_t, \gamma_\times$ ). In the following, we let  $\gamma_a$  and  $\gamma_b$  stand for either of these decompositions. We work in the flat sky approximation throughout, denoting positions on the sky with  $\vec{x}$ .

Let  $\gamma_a(i)$  be the shear component  $a$  measured from galaxy  $i$ . The standard estimator for shear correlation functions  $\xi_{ab} \equiv \langle \gamma_a \gamma_b \rangle$  is given by (e.g., [15]):

$$\hat{\xi}_{ab}(\theta) = \frac{1}{N} \sum_{ij} W^\theta(i, j) w(i) w(j) \gamma_a(i) \gamma_b(j), \quad (3)$$

where the sum runs over all pairs of galaxies  $i, j$ , and the normalization is given by:

$$N = \sum_{ij} W^\theta(i, j) w(i) w(j), \quad (4)$$

where  $w(i)$  is the weight assigned to galaxy  $i$ , and the window function  $W^\theta$  picks out galaxies separated by  $\theta - d\theta \leq |\vec{x}_i - \vec{x}_j| < \theta + d\theta$ . For the remainder of the paper, we will set all weights  $w(i) = 1$ , assuming that they are determined by measurement errors and intrinsic ellipticities [16], and are therefore uncorrelated with the cosmological signal. We also assume that the shape noise is uncorrelated with the density field.

In Appendix B, we consider pixel-based estimators. As shown there, pixel-based estimators for the shear correlation function are subject to a very similar bias to the galaxy pair-based estimator above, provided that each pixel is weighted by inverse variance.

We wish to take the expectation value of equation (3). To do so, we partition the survey volume into infinitesimal cells of equal solid angle  $d\Omega$  so that the number of galaxies  $n_{\text{obs}}(i)d\Omega$  in cell  $i$  is either 0 or 1 for all cells. Given this partition, we can express equation (3) as:

$$\hat{\xi}_{ab}(\theta) = \frac{1}{N} \sum_{ij} W^\theta(i, j) n_{\text{obs}}(i) d\Omega \gamma_a(i) n_{\text{obs}}(j) d\Omega \gamma_b(j) \quad (5)$$

where the sum is now over all cells. The normalization  $N$  can be similarly rewritten. Now, we have that  $n_{\text{obs}}(i) = \bar{n} (1 + \delta_{\text{obs}}(i))$  where  $\delta_{\text{obs}}(i)$  is the fluctuation in the galaxy density field in cell  $i$ . Inserting these expressions into the above equation and taking the expectation value in the continuum limit, we find (see Appendix A for details):

$$\langle \hat{\xi}_{ab}(\theta) \rangle = \left\langle \frac{1}{\mathcal{N}} [1 + \delta_{\text{obs}}(1)] \gamma_a(1) [1 + \delta_{\text{obs}}(2)] \gamma_b(2) \right\rangle, \quad (6)$$

where we have denoted two positions separated by  $\theta$  on the sky with ‘1’ and ‘2’. The quantity  $\mathcal{N}$  is defined in Appendix A and comes from the normalization by the observed number of galaxy pairs.

The important point to note here is the fact that the non-uniform sampling of source galaxies through  $1 + \delta_{\text{obs}}$  makes the estimator in equation (3) sensitive not only to the shear but also to the source galaxy overdensity *and* the lensing magnification. Operationally (with the caveat of higher-order corrections), the estimator in equation (3) replaces the true shear  $\gamma(i)$  by an ‘observed’ shear:

$$\gamma_a^{\text{obs}} \rightarrow \gamma_a (1 + \delta_{\text{obs}}) = \gamma_a (1 + \delta_g + q\kappa). \quad (7)$$

Hence, by expansion of equation (6) we obtain the leading corrections:

$$\begin{aligned} \langle \hat{\xi}_{ab}(\theta) \rangle &= \langle \gamma_a(1) \gamma_b(2) \rangle \\ &+ \langle [\delta_g(1) + q\kappa(1)] \gamma_a(1) \gamma_b(2) \rangle + \langle \gamma_a(1) [\delta_g(2) + q\kappa(2)] \gamma_b(2) \rangle \end{aligned} \quad (8)$$

The correction terms are of two kinds: one involves correlations of  $\delta_g \gamma_a$ , i.e. intrinsic overdensities of background galaxies with shear by mass fluctuations in the foreground. For a sufficiently narrow redshift distribution of source

galaxies, this source-lens clustering is negligible, since the distribution of sources and lenses do not overlap in this case. In case of the lensing skewness and kurtosis, it was shown that the effect is small if the width of the source redshift distribution is less than 0.15 [17]. Hence, if photometric redshifts are available, source-lens clustering can be avoided. We will not further consider source-lens clustering in the main part of the paper.

The second type of correction in equation (8) is due to magnification and size bias and is of the form  $q \cdot \kappa \gamma_a$ . These corrections can be significant, since they correlate the shear field with the *same* foreground lensing field. It is worth noting that the leading lensing bias corrections are of exactly the same form as the reduced shear correction [12, 18, 19]: there,  $\gamma \rightarrow \gamma(1 + \kappa)$  perturbatively, whereas here, we have  $\gamma \rightarrow \gamma(1 + q \kappa)$ . Hence, reduced shear corrections and lensing bias corrections should be considered jointly. The main difference is that the size of lensing bias corrections depends on the background galaxy sample via the parameter  $q$ . From now on, we consider both effects simultaneously, so that:

$$\gamma_a^{\text{obs}} \rightarrow \gamma_a [1 + (1 + q)\kappa]. \quad (9)$$

Note that the normalization  $\mathcal{N}$  in equation (6) is relevant in canceling some higher-order terms. In particular, one might wonder whether the term:

$$\langle \delta_g(1) \delta_g(2) \rangle \langle \gamma_a(1) \gamma_b(2) \rangle, \quad (10)$$

which appears in the expansion of equation (6) might be a significant contribution. This term is however canceled through  $\mathcal{N}$ , since the shear estimator is normalized to the number of observed galaxy pairs used in the measurement (see also Appendix C). The contributing higher-order terms due to lensing bias which we neglected in equation (8) involve the shear 4-point functions. We discuss these terms in Appendix C and find that they are suppressed by roughly two orders of magnitude with respect to the cubic terms, i.e. they entail corrections at the level of  $\mathcal{O}(10^{-4})$  of the shear power spectrum. Corrections of this magnitude are not expected to be of interest in the foreseeable future, hence we neglect them for the remainder of the paper.

### III. IMPACT ON THE POWER SPECTRUM

In this section, we present the results of a calculation of the leading magnification effects on the shear auto-correlation, equation (8). Specifically, we will consider  $\xi_\gamma \equiv \langle \gamma \gamma^* \rangle = \langle \gamma_1 \gamma_1^* \rangle + \langle \gamma_2 \gamma_2^* \rangle$  for background galaxies at a fixed redshift of  $z_s = 1$ . The cubic corrections involve three-point functions of shear and convergence. It is much more convenient to calculate these in Fourier space where, in the absence of B modes, the complex shear is related to the convergence as:

$$\gamma(\vec{\ell}) = e^{2i\phi_\ell} \kappa(\vec{\ell}). \quad (11)$$

Here,  $\phi_\ell$  is the angle of the  $\vec{\ell}$  vector with the  $\vec{x}$ -axis of the coordinate system. Then, the shear power coefficients  $C^\kappa(\ell)$  are defined as:

$$\langle \gamma(\vec{\ell}) \gamma^*(\vec{\ell}') \rangle = \langle \kappa(\vec{\ell}) \kappa(-\vec{\ell}') \rangle = (2\pi)^2 \delta_D(\vec{\ell} - \vec{\ell}') C^\kappa(\ell), \quad (12)$$

and their relation to the real-space correlation function is given by:

$$C^\kappa(\ell) = \int d^2\theta \xi_\gamma(\theta) e^{-i\vec{\ell}\cdot\vec{\theta}}. \quad (13)$$

The calculation then proceeds exactly as in the case of the reduced shear correction [12, 18, 19]. In Fourier space, the multiplication in equation (9) turns into a convolution:

$$(\kappa\gamma)(\vec{\ell}) = \int \frac{d^2\ell_1}{(2\pi)^2} \gamma(\vec{\ell}_1) \kappa(\vec{\ell} - \vec{\ell}_1) = \int \frac{d^2\ell_1}{(2\pi)^2} e^{i2\phi_{\ell_1}} \kappa(\vec{\ell}_1) \kappa(\vec{\ell} - \vec{\ell}_1), \quad (14)$$

where we have used equation (11). Then, the leading correction to the two-point correlator equation (12) is given by:

$$\delta \langle \gamma(\vec{\ell}) \gamma^*(\vec{\ell}') \rangle = 2(1 + q) \int \frac{d^2\ell_1}{(2\pi)^2} e^{i2\phi_{\ell_1}} e^{-i2\phi_{\ell_1'}} \langle \kappa(\vec{\ell}_1) \kappa(\vec{\ell} - \vec{\ell}_1) \kappa(-\vec{\ell}') \rangle, \quad (15)$$

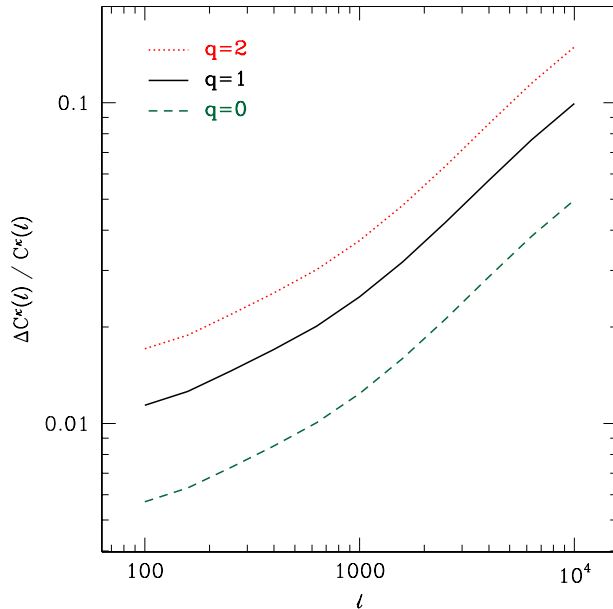


FIG. 1: Relative size of the combined lensing bias and reduced shear correction  $\Delta C^\kappa(\ell)$  on the shear power, for different values of the flux/size count slope  $q$ . The curve for  $q = 0$  only shows the reduced shear correction. A single source redshift  $z_s = 1$  was assumed.

where the factor of 2 comes from the two permutations. Using the definition of the convergence bispectrum,

$$\left\langle \kappa(\vec{\ell}_1)\kappa(\vec{\ell}_2)\kappa(\vec{\ell}_3) \right\rangle = (2\pi)^2 \delta(\vec{\ell}_1 + \vec{\ell}_2 + \vec{\ell}_3) B^\kappa(\ell_1, \ell_2, \ell_3), \quad (16)$$

we obtain the correction to the shear power spectrum:

$$\Delta C^\kappa(\ell) \equiv C_{\text{corr}}^\kappa(\ell) - C^\kappa(\ell) = 2(1+q) \int \frac{d^2\ell_1}{(2\pi)^2} e^{2i(\phi_{\ell_1} - \phi_\ell)} B^\kappa(\vec{\ell}_1, \vec{\ell} - \vec{\ell}_1, -\vec{\ell}). \quad (17)$$

The imaginary part of equation (17) vanishes, signaling that no B modes are produced by these 3-point terms (see Appendix D for a treatment of the B-modes induced by the 4-point terms). The remaining real part is:

$$\Delta C^\kappa(\ell) = 2(1+q) \int \frac{d^2\ell_1}{(2\pi)^2} \cos 2\phi_{\ell_1} B^\kappa(\vec{\ell}_1, \vec{\ell} - \vec{\ell}_1, -\vec{\ell}) \quad (18)$$

Here, we have set  $\phi_\ell = 0$  without loss of generality. The prefactor  $1+q$  in equation (18) sums up the reduced shear and lensing bias corrections.

To estimate  $\Delta C^\kappa(\ell)$ , we adopt a flat  $\Lambda$ CDM cosmology with parameters given by  $h = 0.7$ ,  $\Omega_m = 1 - \Omega_\Lambda = 0.28$ ,  $n_s = 0.96$ ,  $\sigma_8 = 0.85$ . We use equations (C17)–(C18) in Appendix C relating the shear power and bispectrum to the matter power spectrum and bispectrum. Further, we use the non-linear matter power spectrum according to [21] together with the bispectrum fitting formula from [22]. Our calculation of the reduced shear correction agrees with that of [12, 19] where it was shown to match the results of ray-tracing through N-body simulations.

Figure 1 shows the relative magnitude of the cubic correction  $\Delta C^\kappa(\ell)/C^\kappa(\ell)$  from equation (18) for a range of  $q$  values from 0 to 2, for a fixed source redshift of  $z_s = 1$ . In Schmidt et al. [14], we consider a galaxy sample similar to the one expected for the Dark Energy Survey [DES, 23]. Measuring the slope of the galaxy size and magnitude distributions according to equation (2) for a range of magnitude and size cut values, we obtain  $q \approx 1 - 2$  (see [14] for details).

At  $\ell \sim 1000$ , the cubic correction term reaches about 4% for  $q = 2$ , which is larger than what one might naively expect from perturbation theory. This is because of a much larger weighting of low-redshift contributions in the weak lensing bispectrum when compared to the power spectrum (Appendix C): the correction equation (18) is enhanced by the more strongly non-linear matter distribution at low  $z$ .

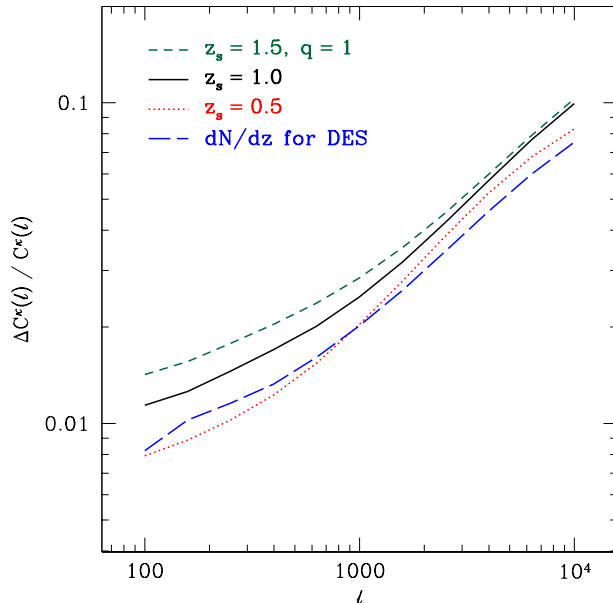


FIG. 2: Same as figure 1, except for different source redshift distributions: the lines for  $z = 0.5$ ,  $z = 1.0$  and  $z = 1.5$  show the result for single source redshifts, while the blue dashed line shows the result for a broad redshift distribution  $z = 0 - 1.4$  expected for the full DES galaxy sample [20].

We show the effect of varying source redshifts in figure 2. The relative correction to  $C^\kappa(\ell)$  increases with redshift, although the  $z$ -dependence is quite weak. We also consider a very broad galaxy redshift distribution  $dN/dz$  expected for the full DES galaxy sample [20], spanning redshifts from 0 to 1.4. Even in this case, the magnitude of the effect is not affected significantly.

#### IV. LENSING BIAS CORRECTIONS TO OTHER SHEAR OBSERVABLES

While we chose the cosmic shear power spectrum as a representative example to illustrate the magnification and size bias effects, it is worth considering briefly the effects on other observables. In the following, we assume values of  $q = 1 - 2$  as typical.

##### A. Mean Shear

Lensing bias (and reduced shear) do not affect the mean of the shear, or convergence if the convergence is estimated from the shear. That is, one might worry that, since regions of large  $\kappa$  are preferentially selected, the average value of the shear in all pixels in a survey might be pushed to a non-zero value. This is not the case. Consider the estimator for the convergence:

$$\kappa^{\text{obs}}(\vec{x}) = \int \frac{d^2\ell}{(2\pi)^2} e^{i\vec{\ell}\cdot\vec{x}} \int d^2x' e^{-i\vec{\ell}\cdot\vec{x}'} [\cos(2\phi_\ell)\gamma_1^{\text{obs}}(\vec{x}') + \sin(2\phi_\ell)\gamma_2^{\text{obs}}(\vec{x}')] \quad (19)$$

where  $\phi_\ell$  is the angle between  $\vec{\ell}$  and the  $x$ -axis, and  $\gamma_a^{\text{obs}}(\vec{x})$  are the measured ellipticities. We have argued that inevitably

$$\gamma_a^{\text{obs}}(\vec{x}) \rightarrow \gamma_a(\vec{x}) [1 + \delta_{\text{obs}}] \quad (20)$$

so contains quadratic terms such as  $\gamma_a(\vec{x})\kappa(\vec{x})$ . Symmetry though dictates that the means of these terms,  $\langle \gamma_a(\vec{x}')\kappa(\vec{x}') \rangle$ , in equation (19) vanish:  $\gamma_1$  is just as likely to be positive as negative so  $\gamma_1\kappa$  averages to zero. The mean therefore of any *linear* combination of the shear components remains zero in the presence of the corrections considered here.

## B. B-Modes

Cooray and Hu [24] pointed out that corrections to the Born approximation inevitably lead to non-zero B-modes. Lensing bias (and reduced shear) also produce B-modes; the Gaussian contribution to the spectrum is (see Appendix D):

$$C^B(\ell) = (1+q)^2 \int \frac{d^2\ell'}{(2\pi)^2} \sin(2\phi_{\ell'}) C^\kappa(\ell') C^\kappa(|\vec{\ell} - \vec{\ell}'|) \left[ \sin(2\phi_{\ell'}) + \sin(2\phi_{\vec{\ell}' - \vec{\ell}}) \right]. \quad (21)$$

Apart from geometric factors and the prefactor, this is of order  $l^2 C^\kappa(l) \sim 10^{-4}$  smaller than the E-mode spectrum, in qualitative agreement with the terms analyzed in [24]. While the factor of  $(1+q)^2$  could provide a boost of order 10 to this B-mode power spectrum, the amplitude is still likely too small to be detected in upcoming surveys. Therefore, B-modes will continue to serve as excellent checks of systematic effects. Note that on very small scales, the non-Gaussian contribution from the trispectrum might be significant. A calculation of this contribution is much more involved and is left for future work.

## C. Galaxy-shear correlation

Following an argument analogous to the one presented for the shear-shear correlation function, we can derive the impact of lensing bias on the galaxy-shear correlation function. The equivalent of equation (6) for the correlation of a background shear  $\gamma_a$  with foreground galaxies is:

$$\langle \hat{\xi}_{ga}(\theta) \rangle = \left\langle \frac{1}{\mathcal{N}'} \delta_{\text{obs}}^{\text{fg}}(1) [1 + \delta_{\text{obs}}(2)] \gamma_a(2) \right\rangle, \quad (22)$$

where  $\mathcal{N}'$  again is from the normalizing denominator in the estimator defined in Appendix A. Expanding equation (22), we obtain the following corrections to the galaxy-shear correlation:

$$\begin{aligned} \langle \hat{\xi}_{ga}(\theta) \rangle &= \langle \delta_g^{\text{fg}}(1) \gamma_a(2) \rangle + q^{\text{fg}} \langle \kappa^{\text{fg}}(1) \gamma_a(2) \rangle \\ &+ \langle [\delta_g^{\text{fg}}(1) + q^{\text{fg}} \kappa^{\text{fg}}(1)] \delta_g(2) \gamma_a(2) \rangle \\ &+ q \langle [\delta_g^{\text{fg}}(1) + q^{\text{fg}} \kappa^{\text{fg}}(1)] \kappa(2) \gamma_a(2) \rangle \end{aligned} \quad (23)$$

Here,  $q^{\text{fg}}$  and  $\kappa^{\text{fg}}$  denote  $q$  and convergence for the foreground galaxies. The first line of equation (23) shows the lowest order contributions, including the lensing bias of foreground galaxies [25, 26], while the second line shows the corrections due to source-lens clustering which we again assume to be small. Finally, the third line shows the contributions due to lensing effects on the background shear. These are again similar to the corresponding reduced shear correction, apart from the factor of  $q$ . In total, we expect the lensing bias effects on the galaxy-shear correlation to be of similar size as those on the shear autocorrelation (Section III), and to scale similarly with redshift.

## D. Shear tomography

Measuring shear correlations between different redshift slices allows for precise constraints on the expansion history of the Universe and the dark energy equation of state,  $w$ . Using the Fisher matrix technique, Shapiro [19] estimated the dark energy parameter biases incurred when neglecting the reduced shear correction. Since the change to the shear-shear power spectrum due to reduced shear and lensing bias scales as  $1+q$ , we expect the corresponding parameter biases to increase by a factor of 2–3 for  $q = 1-2$  if these effects are neglected. For example, for a DES-like survey (DETF Stage-III), we expect a biasing of  $w$  at the 2–3  $\sigma$  level for a flat  $w$ CDM model.

## E. Shear variance and aperture mass

Apart from the correlation function, shear auto-correlations are often measured in terms of top-hat variance  $\gamma_\theta$  and aperture mass  $M_{\text{ap}}(\theta)$  (e.g., [15, 27]). These estimators use window functions which weight angular scales in different ways. White [28] showed that the reduced shear correction has a  $\sim 12\%$  effect on the top-hat shear variance even on large scales. This is because small scales contribute strongly to the shear variance. Following the results of

the previous section, we expect this effect to be amplified by  $(1 + q)$  to a total of  $\sim 24 - 36\%$  when including both reduced shear and lensing bias. In case of the aperture mass, angular scales much smaller than the filter scale are downweighted, so that the effect on the aperture mass variance is smaller; we expect a  $\sim 10 - 25\%$  correction for  $\theta \lesssim 4$  arcmin.

## V. CONCLUSIONS

Estimates of cosmic shear suffer from lensing bias: the way one selects galaxies to estimate shear is correlated with the shear field itself. This correlation reflects the fact that cosmic shear and magnification are due to the same foreground matter along the line of sight, and magnification and size bias can scatter source galaxies into or out of the galaxy catalog.

Lensing bias needs to be understood if lensing is to be used as a precision probe of the dark sector. We estimated that neglecting lensing bias and its cousin reduced shear when interpreting the results of a DETF Stage III cosmic shear experiment such as DES will lead to estimates of the dark energy equation of state which differ from the true value by 2-3 statistical standard deviations. Thus, this is an important systematic that needs to be addressed. In fact, lensing bias is likely to pollute other lensing measures even more severely: piggy-backing on the calculation of [28] for reduced shear alone, we estimate that lensing bias + reduced shear will affect shear variance and aperture mass variance at the 20 – 30% level. This could well be of importance to weak-lensing selected clusters, since cluster finding and mass estimates from weak lensing are based on estimators similar to aperture mass or top hat variance [29, 30]. Lensing bias is also likely to be the most significant source of cosmological B-modes in the shear field, at roughly  $\sim 10^{-3}$  of the E-modes on small scales for the Gaussian contribution.

Correcting for these biases should not be too difficult: the perturbative calculation presented here has been shown to agree with simulations [12]. While better calibration is needed, this is clearly a solvable problem, especially on large scales where baryons are not a factor. Moreover, one can imagine calibrating from the data itself by varying size and magnitude cuts to isolate  $q$ . Indeed, one possible application of lensing bias is as a calibrator for multiplicative and additive shear errors. We plan to explore this possibility in future work.

## Acknowledgments

We would like to thank Chaz Shapiro for helping us in cross-checking our calculations, and Jim Annis for providing the galaxy redshift distribution from DES mock catalogs. In addition, we are grateful to Wayne Hu and Andrew Zentner for helpful discussions.

This work was supported by the Kavli Institute for Cosmological Physics at the University of Chicago through grants NSF PHY-0114422 and NSF PHY-0551142, and by the US Department of Energy, including grants DE-FG02-95ER40896 and DE-FG02-92-ER40699. LH acknowledges support by the Initiatives in Science and Engineering Program at Columbia University. ER was funded by the Center for Cosmology and Astro-Particle Physics (CCAPP) at The Ohio State University, and by NSF grant AST 0707985. ES is supported by DOE grant DE-AC02-98CH10886.

## APPENDIX A: RIGOROUS DERIVATION OF SHEAR CORRECTIONS

This section presents derivations of the exact expressions for the lensing bias and source clustering contributions to shear correlations. To keep the expressions as general as possible, it is useful to define a window function  $W^\theta(\vec{x}, \vec{x}')$ , where  $\vec{x}, \vec{x}'$  stand for positions on the sky, which is normalized so that:

$$\int d^2 x' W^\theta(\vec{x}, \vec{x}') = 1. \quad (\text{A1})$$

In the case of correlation functions,  $W^\theta$  picks out galaxies separated by  $\theta \pm d\theta$ . More generally, other shear observables such as top-hat variance or aperture mass can also be written in this way. Again, we write the un-pixelized estimators



for the shear-shear correlation,  $\hat{\xi}_{ab}(\theta)$  [equation (5)], and the galaxy-shear correlation,  $\hat{\xi}_{ga}(\theta)$  (see Section IV C) as:

$$\hat{\xi}_{ab}(\theta) = \frac{1}{N} \sum_{ij} W^\theta(i, j) n_{\text{obs}}(i) d\Omega \gamma_a(i) n_{\text{obs}}(j) d\Omega \gamma_b(j) \quad (\text{A2})$$

$$N = \sum_{ij} W^\theta(i, j) n_{\text{obs}}(i) d\Omega n_{\text{obs}}(j) d\Omega, \quad (\text{A3})$$

$$\hat{\xi}_{ga}(\theta) = \sum_{ij} W^\theta(i, j) \frac{n_{\text{obs}}(i)}{N'(i)} d\Omega \gamma_a(i) \frac{n_{\text{obs}}^{\text{fg}}(j) - \bar{n}^{\text{fg}}}{\bar{n}^{\text{fg}}} d\Omega, \quad (\text{A4})$$

$$N'(i) = \sum_j W^\theta(i, j) n_{\text{obs}}(j) d\Omega. \quad (\text{A5})$$

We now take the infinitesimal patches of equations (A2)–(A5) to the continuum limit, so that  $n_{\text{obs}}(i)$  becomes  $\bar{n}[1 + \delta_{\text{obs}}(\vec{x})]$ , and write the estimators for galaxy-shear and shear-shear correlations as integrals:

$$\hat{\xi}_{ab}(\theta) = \frac{\int d^2x \int d^2x' [1 + \delta_{\text{obs}}(\vec{x})] \gamma_a(\vec{x}) [1 + \delta_{\text{obs}}(\vec{x}')] \gamma_b(\vec{x}') W^\theta(\vec{x}, \vec{x}')}{\int d^2x'' \int d^2x''' [1 + \delta_{\text{obs}}(\vec{x}'')] [1 + \delta_{\text{obs}}(\vec{x}''')] W^\theta(\vec{x}'', \vec{x}''')} \quad (\text{A6})$$

$$\hat{\xi}_{ga}(\theta) = \int \frac{d^2x}{\Delta\Omega} \int d^2x' \delta_{\text{obs}}^{\text{fg}}(\vec{x}) \frac{[1 + \delta_{\text{obs}}(\vec{x}')] \gamma_a(\vec{x}')}{\int d^2x'' [1 + \delta_{\text{obs}}(\vec{x}'')] W^\theta(\vec{x}, \vec{x}'')} W^\theta(\vec{x}, \vec{x}') \quad (\text{A7})$$

The exact expressions for the expectation values of these estimators are given by:

$$\langle \hat{\xi}_{ab}(\theta) \rangle = \int \frac{d^2x}{\Delta\Omega} \int d^2x' \left\langle \frac{[1 + \delta_{\text{obs}}(\vec{x})] \gamma_a(\vec{x}) [1 + \delta_{\text{obs}}(\vec{x}')] \gamma_b(\vec{x}')}{\int d^2x'' / \Delta\Omega \int d^2x''' [1 + \delta_{\text{obs}}(\vec{x}'')] [1 + \delta_{\text{obs}}(\vec{x}''')] W^\theta(\vec{x}'', \vec{x}''')} \right\rangle W^\theta(\vec{x}, \vec{x}') \quad (\text{A8})$$

$$\langle \hat{\xi}_{ga}(\theta) \rangle = \int \frac{d^2x}{\Delta\Omega} \int d^2x' \left\langle \frac{\delta_{\text{obs}}^{\text{fg}}(\vec{x}) [1 + \delta_{\text{obs}}(\vec{x}')] \gamma_a(\vec{x}')}{\int d^2x'' [1 + \delta_{\text{obs}}(\vec{x}'')] W^\theta(\vec{x}, \vec{x}'')} \right\rangle W^\theta(\vec{x}, \vec{x}') \quad (\text{A9})$$

Now we neglect the integrals outside of the correlators, which essentially smooth the correlation functions over the separations defined by the angular bin width. Using some additional notation, we can then write the expectation values of the quadratic estimators as follows:

$$\langle \hat{\xi}_{ab}(\theta) \rangle = \left\langle \frac{[1 + \delta_{\text{obs}}(1)] \gamma_a(1) [1 + \delta_{\text{obs}}(2)] \gamma_b(2)}{1 + 2\overline{\delta_{\text{obs}}} + \widehat{\delta_{\text{obs}}\delta_{\text{obs}}}} \right\rangle \quad (\text{A10})$$

$$\langle \hat{\xi}_{ga}(\theta) \rangle = \left\langle \frac{\delta_{\text{obs}}^{\text{fg}}(1) [1 + \delta_{\text{obs}}(2)] \gamma_a(2)}{1 + \overline{\delta_{\text{obs}}(1)}} \right\rangle, \quad (\text{A11})$$

where we have defined:

$$\widehat{\delta_{\text{obs}}}(\vec{x}) \equiv \int d^2x' \delta_{\text{obs}}(\vec{x}') W^\theta(\vec{x}, \vec{x}') \quad (\text{A12})$$

$$\overline{\delta_{\text{obs}}} \equiv \int \frac{d^2x}{\Delta\Omega} \delta_{\text{obs}}(\vec{x}) \quad (\text{A13})$$

$$\widehat{\delta_{\text{obs}}\delta_{\text{obs}}} \equiv \int \frac{d^2x}{\Delta\Omega} \int d^2x' \delta_{\text{obs}}(\vec{x}) \delta_{\text{obs}}(\vec{x}') W^\theta(\vec{x}, \vec{x}') \quad (\text{A14})$$

The first quantity is the observed overdensity averaged over an annulus around the given location. Hence, it is evaluated at position ‘1’, giving the overdensity of observed galaxies in an annulus around that position. For sufficiently large separations  $\theta$ ,  $\widehat{\delta_{\text{obs}}}$  will be small, while it will be of order unity for separations close to the galaxy correlation length.  $\overline{\delta_{\text{obs}}}$  is the overdensity of the galaxy sample (including magnification) averaged over the whole survey, measured relative to the ensemble average or an infinite-volume survey. We have not neglected this averaged overdensity for the sake of completeness, although for actual wide-field surveys this will be negligible. Finally,  $\widehat{\delta_{\text{obs}}\delta_{\text{obs}}}$  is a product of overdensities smoothed over separations around  $\theta$ . Note that this quantity is within the expectation value and hence cannot immediately be replaced by  $\xi_{gg}(\theta)$ .



We now expand the expectation values of the correlation functions up to fourth order in  $\delta$  and  $\kappa$ . For sake of brevity, we keep  $\delta_{\text{obs}}$  [equation (1)] unexpanded:

$$\begin{aligned} \langle \hat{\xi}_{ab}(\theta) \rangle &= \langle \gamma_a(1)\gamma_b(2) \rangle \\ &+ \langle [\delta_{\text{obs}}(1) - \overline{\delta_{\text{obs}}}] \gamma_a(1)\gamma_b(2) \rangle + \langle \gamma_a(1) [\delta_{\text{obs}}(2) - \overline{\delta_{\text{obs}}}] \gamma_b(2) \rangle \\ &+ \langle [\delta_{\text{obs}}(1)\delta_{\text{obs}}(2) - \widehat{\delta_{\text{obs}}\delta_{\text{obs}}}] \gamma_a(1)\gamma_b(2) \rangle \\ &- 2\langle \overline{\delta_{\text{obs}}} [\delta_{\text{obs}}(1) + \delta_{\text{obs}}(2)] \gamma_a(1)\gamma_b(2) \rangle + 2\langle \overline{\delta_{\text{obs}}^2} \gamma_a(1)\gamma_b(2) \rangle \end{aligned} \quad (\text{A15})$$

$$\begin{aligned} \langle \hat{\xi}_{ga}(\vartheta) \rangle &= \langle \delta_{\text{obs}}^{\text{fg}}(1)\gamma_a(2) \rangle \\ &+ \langle \delta_{\text{obs}}^{\text{fg}}(1) [\delta_{\text{obs}}(2) - \widetilde{\delta_{\text{obs}}}(1)] \gamma_a(2) \rangle \\ &+ \langle \delta_{\text{obs}}^{\text{fg}}(1) [\widetilde{\delta_{\text{obs}}^2}(1) - \widetilde{\delta_{\text{obs}}}(1)\delta_{\text{obs}}(2)] \gamma_a(2) \rangle \end{aligned} \quad (\text{A16})$$

To be explicit, the term in the third line for  $\xi_{ab}$  stands for:

$$\int d^2x_1 \int d^2x_2 W^\theta(\vec{x}_1, \vec{x}_2) \left\langle \left[ \delta_{\text{obs}}(\vec{x}_1) \delta_{\text{obs}}(\vec{x}_2) - \int d^2x_3 \int d^2x_4 W^\theta(\vec{x}_3, \vec{x}_4) \delta_{\text{obs}}(\vec{x}_3) \delta_{\text{obs}}(\vec{x}_4) \right] \gamma_a(\vec{x}_1) \gamma_b(\vec{x}_2) \right\rangle \quad (\text{A17})$$

Note that the form of all magnification/size bias corrections in the final expressions correspond to a replacement of the form:

$$\gamma(1) \rightarrow \gamma(1) \{1 + \delta_{\text{obs}}(1) - S[\delta_{\text{obs}}](1)\}, \text{ etc.}, \quad (\text{A18})$$

where  $S[\delta_{\text{obs}}]$  is some smoothing of  $\delta_{\text{obs}}$  over annuli or the whole survey. Hence, all corrections vanish if either,  $\delta_{\text{obs}} = S[\delta_{\text{obs}}]$ , i.e. there is no observed clustering of background galaxies (including magnification effects), or if the shear field  $\gamma$  is uncorrelated with  $\delta_{\text{obs}}$ . This holds analogously for a pixelized estimator (see Appendix B) and is in line with the intuitive understanding of the magnification corrections. Keeping only the cubic terms of equation (A15), and neglecting  $\overline{\delta_{\text{obs}}}$ , we arrive at equation (8). See Appendix C for a discussion of the four-point terms.

## APPENDIX B: PIXEL-BASED SHEAR ESTIMATORS

An alternative approach to estimating shear correlations is to divide the survey volume into pixels  $\alpha$  of finite volume defined by window functions  $\mathcal{W}_\alpha(\vec{x})$  (normalized so that  $\int \mathcal{W}_\alpha(\vec{x}) d^2x = 1$ ). Each pixel contains many galaxies, and one estimates the shear and galaxy overdensity directly for each pixel (e.g., [15, 31]; again setting all weights to 1):

$$\hat{\gamma}_a(\alpha) = \frac{1}{n_{\text{pix}}(\alpha)} \sum_i n_{\text{obs}}(i) \gamma_a(i) \mathcal{W}_\alpha(i) \quad (\text{B1})$$

$$\hat{\delta}(\alpha) = \frac{n_{\text{pix}}^{\text{fg}}(\alpha)}{\bar{n}_{\text{pix}}^{\text{fg}}} - 1 = \sum_i \frac{n_{\text{obs}}^{\text{fg}}(i) - \bar{n}_{\text{pix}}^{\text{fg}}}{\bar{n}_{\text{pix}}^{\text{fg}}} \mathcal{W}_\alpha(i) \quad (\text{B2})$$

Here,  $\gamma_a(i)$  is the shear measured from galaxy  $i$ ,  $n_{\text{obs}}^{\text{fg}}$  is the *foreground* galaxy density, and we have again subdivided the finite-sized pixel into infinitesimal patches  $i$ , so that the observed number of galaxies  $n_{\text{obs}}(i)$  in each patch is either 0 or 1.  $n_{\text{pix}}(\alpha)$  is the number of galaxies observed in pixel  $\alpha$ , while  $\bar{n}_{\text{pix}}$  is the expected average number of galaxies per pixel:

$$n_{\text{pix}}(\alpha) = \sum_i n_{\text{obs}}(i) \mathcal{W}_\alpha(i), \quad \bar{n}_{\text{pix}} = \sum_i \bar{n} \mathcal{W}_\alpha(i) = \bar{n}, \quad (\text{B3})$$

and analogously for the foreground galaxy densities. The estimators equation (B1) and (B2) result in pixelized maps of the shear components and foreground galaxy overdensities, which can then be processed in real or Fourier space to measure shear correlations.

Going to the continuum limit of equation (B1) and (B2) yields:

$$\hat{\gamma}_a(\alpha) = \frac{\int d^2x [1 + \delta_{\text{obs}}(\vec{x})] \gamma_a(\vec{x}) \mathcal{W}_\alpha(\vec{x})}{\int d^2x' [1 + \delta_{\text{obs}}(\vec{x}')] \mathcal{W}_\alpha(\vec{x}')} \quad (\text{B4})$$

$$\hat{\delta}(\alpha) = \int d^2x \frac{n_{\text{obs}}^{\text{fg}}(\vec{x}) - \bar{n}_{\text{pix}}^{\text{fg}}}{\bar{n}_{\text{pix}}^{\text{fg}}} \mathcal{W}_\alpha(\vec{x}), \quad \bar{n}_{\text{pix}}^{\text{fg}} = \int \frac{d^2x}{\Delta\Omega} n_{\text{obs}}(\vec{x}) \quad (\text{B5})$$

We now take expectation values of correlators of the pixelized shear and overdensity fields, neglecting the effect of pixelization on the correlation function (which is appropriate if the separation  $\theta$  is much larger than the pixel scale):

$$\langle \hat{\xi}_{ab}(\theta) \rangle = \left\langle \frac{(1 + \overline{\delta_{\text{obs}}})\overline{\gamma}_a(1)}{1 + \overline{\delta_{\text{obs}}}(1)} \frac{(1 + \overline{\delta_{\text{obs}}})\overline{\gamma}_b(2)}{1 + \overline{\delta_{\text{obs}}}(2)} \right\rangle \quad (\text{B6})$$

$$\langle \hat{\xi}_{ga}(\theta) \rangle = \left\langle \frac{\overline{\delta_{\text{obs}}^{\text{fg}}}(1)}{\overline{\delta_{\text{obs}}}(1)} \frac{(1 + \overline{\delta_{\text{obs}}})\overline{\gamma}_a(2)}{1 + \overline{\delta_{\text{obs}}}(2)} \right\rangle, \quad (\text{B7})$$

where we have labeled two points separated by  $\theta$  as 1 and 2. Here, barred quantities denote averages over pixels:

$$\overline{X}(\alpha) \equiv \int d^2x' X(\vec{x}') \mathcal{W}_\alpha(\vec{x}'). \quad (\text{B8})$$

In equation (B7), we have neglected a correction due to the integral constraint [32], since  $\bar{n}$  is measured in the survey itself. However, this effect is of order the overdensity averaged over the whole survey, and hence very small for large surveys. In contrast, the denominators kept in equations (B6)–(B7) are integral constraints which are important, since they are of order of the overdensity averaged over *pixel* scales.

Expanding the expectation values to fourth order, we obtain for the pixelized estimators:

$$\begin{aligned} \langle \hat{\xi}_{ab}(\theta) \rangle &= \langle \overline{\gamma}_a(1)\overline{\gamma}_b(2) \rangle \\ &+ \langle \overline{\gamma}_a(1) [\overline{\delta_{\text{obs}}}\overline{\gamma}_b(2) - \overline{\delta_{\text{obs}}}(2)\overline{\gamma}_b(2)] \rangle + \langle [\overline{\delta_{\text{obs}}}\overline{\gamma}_a(1) - \overline{\delta_{\text{obs}}}(1)\overline{\gamma}_a(1)] \overline{\gamma}_b(2) \rangle \\ &+ \langle [\overline{\delta_{\text{obs}}}\overline{\gamma}_a(1) - \overline{\delta_{\text{obs}}}(1)\overline{\gamma}_a(1)] [\overline{\delta_{\text{obs}}}\overline{\gamma}_b(2) - \overline{\delta_{\text{obs}}}(2)\overline{\gamma}_b(2)] \rangle \\ &+ \left\langle [\overline{\delta_{\text{obs}}^2}(1)\overline{\gamma}_a(1) - \overline{\delta_{\text{obs}}}(1)\overline{\delta_{\text{obs}}}\overline{\gamma}_a(1)] \overline{\gamma}_b(2) \right\rangle + \left\langle \overline{\gamma}_a(1) [\overline{\delta_{\text{obs}}^2}(2)\overline{\gamma}_b(2) - \overline{\delta_{\text{obs}}}(2)\overline{\delta_{\text{obs}}}\overline{\gamma}_b(2)] \right\rangle \end{aligned} \quad (\text{B9})$$

$$\begin{aligned} \langle \hat{\xi}_{ga}(\theta) \rangle &= \left\langle \overline{\delta_{\text{obs}}^{\text{fg}}}(1)\overline{\gamma}_a(2) \right\rangle \\ &+ \left\langle \overline{\delta_{\text{obs}}^{\text{fg}}}(1) [\overline{\delta_{\text{obs}}}\overline{\gamma}_a(2) - \overline{\delta_{\text{obs}}}(2)\overline{\gamma}_a(2)] \right\rangle \\ &+ \left\langle \overline{\delta_{\text{obs}}^{\text{fg}}}(1) [\overline{\delta_{\text{obs}}^2}(2)\overline{\gamma}_a(2) - \overline{\delta_{\text{obs}}}(2)\overline{\delta_{\text{obs}}}\overline{\gamma}_a(2)] \right\rangle \end{aligned} \quad (\text{B10})$$

$$(\text{B11})$$

Clearly, all corrections vanish if  $\overline{\delta_{\text{obs}}}\overline{\gamma} = \overline{\delta_{\text{obs}}}\overline{\gamma}$  within a correlator, which is the case if either the observed galaxy distribution  $\delta_{\text{obs}}$  or the shear  $\gamma$  are smooth on pixel scales, or if they are completely uncorrelated.

For the same reasons as for the unpixelized estimator, detailed in Appendix C, the quartic corrections are much smaller than the cubic corrections. Repeating the derivation leading to equation (18), and noting that in Fourier space the smoothed convergence field is given by:

$$\overline{\kappa}(\vec{\ell}) = \widetilde{\mathcal{W}}(\vec{\ell}) \kappa(\vec{\ell}), \quad \widetilde{\mathcal{W}}(\vec{\ell}) \equiv \int d^2x W_\alpha(\vec{x}) e^{-i\vec{\ell}\cdot\vec{x}}, \quad (\text{B12})$$

we obtain the following expression for the magnification correction to the shear power  $C^\kappa(\ell)$  in case of the pixelized estimator:

$$\Delta C_\ell = 2q \int \frac{d^2\ell_1}{(2\pi)^2} \cos 2\phi_{\ell_1} \left[ \widetilde{\mathcal{W}}(\vec{\ell}) - \widetilde{\mathcal{W}}(\vec{\ell}_1)\widetilde{\mathcal{W}}(-\vec{\ell} - \vec{\ell}_1) \right] B(\vec{\ell}, \vec{\ell}_1, -\vec{\ell} - \vec{\ell}_1) \quad (\text{B13})$$

$$\approx 2q \int \frac{d^2\ell_1}{(2\pi)^2} \cos 2\phi_{\ell_1} \left[ 1 - |\widetilde{\mathcal{W}}(\vec{\ell}_1)|^2 \right] B(\vec{\ell}, \vec{\ell}_1, -\vec{\ell} - \vec{\ell}_1). \quad (\text{B14})$$

For the second approximate equality, we have assumed that  $\ell \ll 1/\theta_{\text{pix}}$ , where  $\theta_{\text{pix}}$  is the angular size of the pixels, so that  $\widetilde{\mathcal{W}}(\vec{\ell}) \approx 1$ . The factor in square brackets in equation (B14) is the only difference in the magnification correction for the pixelized estimator compared to equation (18). This factor acts as a high pass, so that only modes with  $\ell \gtrsim 1/\theta_{\text{pix}}$  contribute to the magnification corrections, as expected from equation (B9) and our discussion above. Hence, for sufficiently small pixels, the magnification corrections are suppressed.

Note, however, that our derivations assumes that in estimating shear correlations from pixelized maps, all pixels receive the same weight. If a weighting scheme according to signal-to-noise is used, weighting each pixel by the number of observed galaxies within the pixel (as appropriate for inverse variance weighting), the magnification correction is re-introduced, and we essentially go back to equation (18). Note that in any case the reduced shear correction is not suppressed by using small pixels, and is always given by equation (18).

### APPENDIX C: QUARTIC CORRECTIONS

Going from equation (A15) to equation (8), we have neglected several 4-point correlations. For the estimators we consider, all of the 4-point terms due to lensing bias are suppressed by roughly two orders of magnitude compared to the cubic terms, as we discuss below. Similar conclusions hold for the 4-point terms in the pixelized estimator. In the following, we again neglect the galaxy overdensity averaged over the whole survey,  $\bar{\delta}_{\text{obs}}$ .

The 4-point contributions can be divided into three classes. First, there are source-lens clustering terms:

$$\Delta \langle \hat{\xi}_{ab}(\theta) \rangle_{\text{quartic,I}} = \langle [\delta_g(1)\delta_g(2) - \widehat{\delta_g\delta_g}] \gamma_a(1)\gamma_b(2) \rangle_{\text{connected}} \quad (\text{C1})$$

$$+ \langle \delta_g(1)\gamma_a(1) \rangle \langle \delta_g(2)\gamma_b(2) \rangle - \langle \widehat{\delta_g\gamma_a(1)} \rangle \langle \delta_g\gamma_b(2) \rangle \quad (\text{C2})$$

$$+ \langle \delta_g(1)\gamma_b(2) \rangle \langle \delta_g(2)\gamma_a(1) \rangle - \langle \widehat{\delta_g\gamma_a(1)} \rangle \langle \delta_g\gamma_b(2) \rangle \quad (\text{C3})$$

$$+ \langle \delta_g(1)\delta_g(2) \rangle \langle \gamma_a(1)\gamma_b(2) \rangle - \langle \widehat{\delta_g\delta_g} \rangle \langle \gamma_a(1)\gamma_b(2) \rangle. \quad (\text{C4})$$

The first, connected term is related to the matter four-point function. The second and third lines contain the actual source-lens terms. Note that for the second terms in each line, the product of the two correlators is to be integrated over following equation (A14). The two terms in the fourth line cancel, since  $\langle \widehat{\delta_g\delta_g} \rangle = \langle \delta_g(1)\delta_g(2) \rangle$  (see equation (A14)). This cancelation is a consequence of the normalizing denominator in equation (A2): when measuring the shear, we divide by the number of pairs of observed galaxies with given separation  $\theta$ .

The second set of quartic contributions are mixed source-lens clustering and lensing bias terms:

$$\Delta \langle \hat{\xi}_{ab}(\theta) \rangle_{\text{quartic,II}} = q \langle [\delta_g(1)\kappa(2) - \widehat{\delta_g\kappa}] \gamma_a(1)\gamma_b(2) \rangle_{\text{connected}} \quad (\text{C5})$$

$$+ q \left\{ \langle \delta_g(1)\gamma_a(1) \rangle \langle \kappa(2)\gamma_b(2) \rangle - \langle \widehat{\delta_g\gamma_a(1)} \rangle \langle \kappa\gamma_b(2) \rangle \right\} \quad (\text{C6})$$

$$+ q \left\{ \langle \delta_g(1)\gamma_b(2) \rangle \langle \kappa(2)\gamma_a(1) \rangle - \langle \widehat{\delta_g\gamma_a(1)} \rangle \langle \kappa\gamma_b(2) \rangle \right\} \quad (\text{C7})$$

$$+ q \left\{ \langle \delta_g(1)\kappa(2) \rangle \langle \gamma_a(1)\gamma_b(2) \rangle - \langle \widehat{\delta_g\kappa} \rangle \langle \gamma_a(1)\gamma_b(2) \rangle \right\} \quad (\text{C8})$$

$$+ \{ \delta_g(1)\kappa(2) \leftrightarrow \kappa(1)\delta_g(2) \}. \quad (\text{C9})$$

As expected, these are all proportional to  $q$ . The first three lines again give the contributing source-lens clustering/lensing bias contributions, while the terms in the fourth line cancel.

Finally, the quartic terms from ‘‘pure’’ lensing bias receive two contributions: first, from the quartic terms in equation (A15). Second, there are quadratic contributions to  $\delta_{\text{obs}}$  from lensing bias. Expanding the lensing magnification  $A = [(1 - \kappa)^2 - |\gamma|^2]^{-1/2}$  to second order, we obtain [33]<sup>1</sup>:

$$\delta_{\text{obs}} = \delta_g + q\kappa + c_1\kappa^2 + c_2|\gamma|^2, \quad (\text{C10})$$

where  $c_1 = q(q+1)/2$ ,  $c_2 = q/2$ , and  $|\gamma|^2 = \gamma_1^2 + \gamma_2^2$ . Together, we obtain the following quartic terms due to lensing bias:

$$\Delta \langle \hat{\xi}_{ab}(\theta) \rangle_{\text{quartic,III}} = q^2 \langle [\kappa(1)\kappa(2) - \widehat{\kappa\kappa}] \gamma_a(1)\gamma_b(2) \rangle_{\text{connected}} \quad (\text{C11})$$

$$+ 2q^2 \left\{ \langle \kappa(1)\gamma_a(1) \rangle \langle \kappa(2)\gamma_b(2) \rangle - \langle \widehat{\kappa\gamma_a(1)} \rangle \langle \kappa\gamma_b(2) \rangle \right\} \quad (\text{C12})$$

$$+ q \left\{ \langle \kappa(1)\kappa(2) \rangle \langle \gamma_a(1)\gamma_b(2) \rangle - \langle \widehat{\kappa\kappa} \rangle \langle \gamma_a(1)\gamma_b(2) \rangle \right\} \quad (\text{C13})$$

$$+ c_1 \langle \kappa^2(1)\gamma_a(1)\gamma_b(2) \rangle_{\text{connected}} + c_2 \langle |\gamma(1)|^2 \gamma_a(1)\gamma_b(2) \rangle_{\text{connected}} + \{(1) \leftrightarrow (2)\} \quad (\text{C14})$$

$$+ \{c_1 \langle \kappa^2(1) \rangle + c_2 \langle |\gamma(1)|^2 \rangle\} \langle \gamma_a(1)\gamma_b(2) \rangle + \{(1) \leftrightarrow (2)\} \quad (\text{C15})$$

$$+ 2c_1 \langle \kappa(1)\gamma_a(1) \rangle \langle \kappa(1)\gamma_b(2) \rangle + 2c_2 \sum_{c=1,2} \langle \gamma_c(1)\gamma_a(1) \rangle \langle \gamma_c(1)\gamma_b(2) \rangle + \{(1) \leftrightarrow (2)\}. \quad (\text{C16})$$

<sup>1</sup> We neglect second derivatives of  $n_{\text{obs}}$  with respect to  $\ln f$ ,  $\ln r$  here.

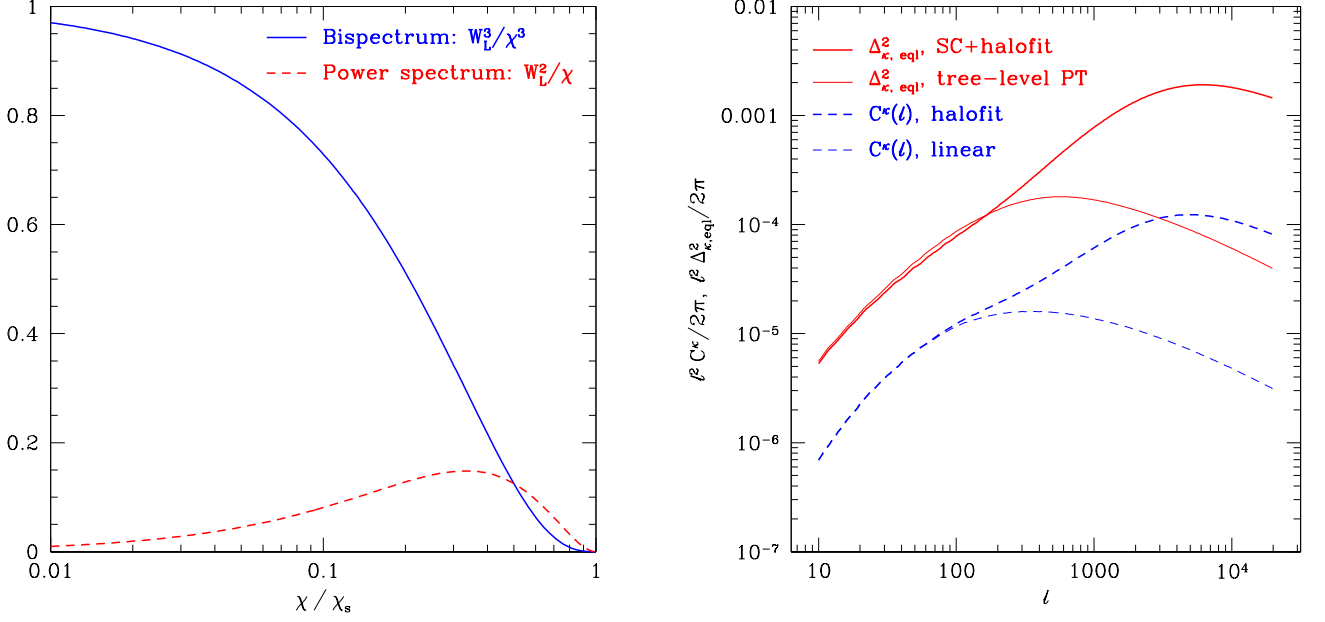


FIG. 3: *Left panel:* Lensing weight functions for the shear power spectrum,  $W_L(\chi_s, \chi)^2/\chi$  (red, dashed), and the shear bispectrum,  $W_L(\chi_s, \chi)^3/\chi^3$  (blue, solid), in units of  $\chi_s$ . *Right panel:* Scaled shear power  $\ell^2/(2\pi) C^\kappa(\ell)$  (blue, dashed), and equilateral bispectrum power  $\ell^2/(2\pi) \sqrt{B^\kappa(\ell, \ell, \ell)}$  (red, solid), for  $z_s = 1$ . The thin lines show the linear/tree-level prediction, while the thick lines are using the non-linear fitting formulas of [21] and [22].

Here,  $\{(1) \leftrightarrow (2)\}$  means that  $\kappa^2(1)$ ,  $|\gamma(1)|^2$  are to be replaced with  $\kappa^2(2)$ ,  $|\gamma(2)|^2$ , respectively. Line (C11) and (C14) are connected terms given by the shear four-point function. We will discuss those below. The terms in line (C13) cancel in the same way as the corresponding source-lens terms. The terms in lines (C12), (C15), (C16) are proportional to  $\xi_{\kappa\kappa}(\theta)^2$ , or  $\xi_{\kappa\kappa}(\theta) \xi_{\kappa\kappa}(0)$ . In other words, the relative magnitude of these corrections is of order  $\xi_{\kappa\kappa}(0) \sim \text{few } 10^{-4}$  or less. Hence, we can safely neglect them compared with the percent-level of the cubic corrections.

In order to understand why the cubic corrections are so much more important, consider the expressions for the shear power spectrum (2-point function) and bispectrum (3-point function). Using the Limber or small-angle approximation, the shear power for sources at a fixed redshift  $z_s$ , with  $\chi_s = \chi(z_s)$ , can be written as a projection of the matter power spectrum  $P(k, \chi)$ :

$$C^\kappa(\ell) = \left( \frac{3}{2} \Omega_m H_0^2 \right)^2 \int_0^{\chi_s} \frac{d\chi}{\chi} \frac{W_L(\chi_s, \chi)^2}{\chi a^2(\chi)} P(\ell/\chi; \chi). \quad (\text{C17})$$

Here,  $\chi$  denotes comoving distance,  $W_L(\chi_s, \chi) = \chi/\chi_s (\chi_s - \chi)$ , and  $a$  is the scale factor. Similarly, the shear bispectrum  $B^\kappa$  can be written as a projection of the matter bispectrum  $B(k_1, k_2, k_3; \chi)$ :

$$B^\kappa(\vec{\ell}_1, \vec{\ell}_2, \vec{\ell}_3) = \left( \frac{3}{2} \Omega_m H_0^2 \right)^3 \int_0^{\chi_s} \frac{d\chi}{\chi} \left( \frac{W_L(\chi_s, \chi)}{\chi a(\chi)} \right)^3 B\left( \frac{\vec{\ell}_1}{\chi}, \frac{\vec{\ell}_2}{\chi}, \frac{\vec{\ell}_3}{\chi}; \chi \right), \quad (\text{C18})$$

In case the sources are distributed according to a broad redshift distribution,  $dN/dz$  (assumed normalized to unity),  $W_L$  in equations (C17)–(C18) is to be replaced with:

$$W_{L, dN/dz}(\chi) = \frac{1}{H(\chi)} \int_{z(\chi)}^\infty dz_s W_L(\chi(z_s), \chi) \frac{dN}{dz}(z_s). \quad (\text{C19})$$

Now, for the 3D matter field,  $\langle \delta(1)\delta(2)\delta(3) \rangle$  is of the same order of magnitude as  $\langle \delta(1)\delta(2) \rangle \langle \delta(2)\delta(3) \rangle + \text{cycl.}$ . However, in case of the shear, which is proportional to the *projected* density field,  $B^\kappa(\ell, \ell, \ell)$  is larger than  $C^\kappa(\ell)^2$  by a factor of order several hundreds (right panel of figure 3). This is because the two-point and three-point functions are projected with a different weighting of low- $z$  contributions. Figure 3 (left panel) shows the effective weight functions for  $C^\kappa$  (red, dashed) and  $B^\kappa$  (blue, solid). Clearly, the late-time contributions receive more weight in case of the bispectrum,

which grows as  $\sim D(a)^4$ . In addition, the low- $z$  contributions along the line of sight are probed at smaller scales, which additionally enhances the bispectrum. For this reason, the cubic corrections dominate the disconnected quartic contributions in equations (C11)–(C16), even though they are formally of the same order in perturbation theory.

The connected four-point terms, equation (C11) and (C14), are given by the convergence trispectrum. We can roughly estimate the contribution from these terms relative to the cubic terms as:

$$\frac{\Delta C_{\text{quartic}}^\kappa(\ell)}{\Delta C_{\text{cubic}}^\kappa(\ell)} \sim \frac{\ell^4 T_{\text{sq}}^\kappa(\ell)}{\ell^2 B_{\text{eq}}^\kappa(\ell)} = 2\pi \frac{(\Delta_{\text{sq}}^2)^3}{(\Delta_{\text{eq}}^2)^2} \lesssim 0.05 \text{ for } \ell \leq 10^4. \quad (\text{C20})$$

Here,  $T_{\text{sq}}^\kappa$  denotes the square trispectrum,  $B_{\text{eq}}^\kappa$  denotes the equilateral bispectrum, and the scaled quantities  $\Delta_{\text{eq}}^2$ ,  $\Delta_{\text{sq}}^2$  were defined and calculated in [34, 35]:

$$\Delta_{\text{eq}}^2(\ell) \equiv \frac{\ell^2}{2\pi} [B_{\text{eq}}^\kappa(\ell)]^{1/2}, \quad \Delta_{\text{sq}}^2(\ell) \equiv \frac{\ell^2}{2\pi} [T_{\text{sq}}^\kappa(\ell)]^{1/3}. \quad (\text{C21})$$

Note that for very small scales, or in case equation (C20) underestimates the size of the connected (non-Gaussian) quartic contributions, the quartic contribution in equation (C11), (C14) are positive and act to increase the magnification corrections.

## APPENDIX D: B-MODES

The new terms induced by lensing bias produce B-modes in addition to the E-modes. This is somewhat akin to the well-known effect of lensing of the cosmic microwave background, when large scale structure distorts the E-modes. Cooray and Hu [24] examined the B-modes induced by higher order corrections to the Born approximation. Lensing bias (and reduced shear) lead to an additional source of B-modes. The estimator for the B-mode is:

$$\hat{B}(\vec{\ell}) = \sin(2\phi_\ell) \gamma_1^{\text{obs}}(\vec{\ell}) - \cos(2\phi_\ell) \gamma_2^{\text{obs}}(\vec{\ell}) \quad (\text{D1})$$

with associated power spectrum:

$$\begin{aligned} C^B(\ell) &= \int \frac{d^2 \ell'}{(2\pi)^2} \langle \hat{B}(\vec{\ell}) \hat{B}(\vec{\ell}') \rangle \\ &= \int \frac{d^2 \ell'}{(2\pi)^2} \langle [\sin(2\phi_\ell) \gamma_1^{\text{obs}}(\vec{\ell}) - \cos(2\phi_\ell) \gamma_2^{\text{obs}}(\vec{\ell})] [\sin(2\phi_{\ell'}) \gamma_1^{\text{obs}}(\vec{\ell}') - \cos(2\phi_{\ell'}) \gamma_2^{\text{obs}}(\vec{\ell}')] \rangle. \end{aligned} \quad (\text{D2})$$

In the absence of lensing corrections,  $\gamma_1^{\text{obs}}(\vec{\ell}) = \cos(2\phi_\ell) \kappa(\vec{\ell})$  and  $\gamma_2^{\text{obs}}(\vec{\ell}) = \sin(2\phi_\ell) \kappa(\vec{\ell})$ , so the power spectrum vanishes identically. Lensing effects lead to a new term when the shears are estimated:

$$\gamma_a^{\text{obs}}(\vec{x}) \rightarrow \gamma_a(\vec{x}) [1 + (1+q)\kappa(\vec{x})] \quad (\text{D3})$$

or in Fourier space,

$$\gamma_a^{\text{obs}}(\vec{\ell}) \rightarrow \gamma_a(\vec{\ell}) + (1+q) \int \frac{d^2 \ell'}{(2\pi)^2} \gamma_a(\vec{\ell}') \kappa(\vec{\ell} - \vec{\ell}'). \quad (\text{D4})$$

The second term here is the only one that survives when computing the B-mode spectrum. Inserting these into equation (D2) leads to

$$\begin{aligned} C^B(\ell) &= (1+q)^2 \int \frac{d^2 \ell'}{(2\pi)^2} \int \frac{d^2 \ell''}{(2\pi)^2} \int \frac{d^2 \ell'''}{(2\pi)^2} \langle [\sin(2\phi_\ell) \cos(2\phi_{\ell''}) \kappa(\vec{\ell}'') \kappa(\vec{\ell} - \vec{\ell}'') - \cos(2\phi_\ell) \sin(2\phi_{\ell''}) \kappa(\vec{\ell}'') \kappa(\vec{\ell} - \vec{\ell}'')] \\ &\quad \times [\sin(2\phi_{\ell'}') \cos(2\phi_{\ell''''}) \kappa(\vec{\ell}''') \kappa(\vec{\ell}' - \vec{\ell}''') - \cos(2\phi_{\ell'}') \sin(2\phi_{\ell''''}) \kappa(\vec{\ell}''') \kappa(\vec{\ell}' - \vec{\ell}''')] \rangle \\ &= (1+q)^2 \int \frac{d^2 \ell'}{(2\pi)^2} \int \frac{d^2 \ell''}{(2\pi)^2} \int \frac{d^2 \ell'''}{(2\pi)^2} \sin(2\phi_\ell - 2\phi_{\ell''}) \sin(2\phi_{\ell'}' - 2\phi_{\ell''''}) \langle \kappa(\vec{\ell}'') \kappa(\vec{\ell} - \vec{\ell}'') \kappa(\vec{\ell}''') \kappa(\vec{\ell}' - \vec{\ell}''') \rangle. \end{aligned} \quad (\text{D5})$$

Apart from the  $l = 0$  mode, there are two ways to contract the (assumed) Gaussian convergence fields in equation (D5)

$$\langle \kappa(\vec{\ell}'') \kappa(\vec{\ell} - \vec{\ell}'') \kappa(\vec{\ell}''') \kappa(\vec{\ell}' - \vec{\ell}''') \rangle = (2\pi)^4 \delta^2(\vec{\ell} + \vec{\ell}') C^\kappa(\ell'') C^\kappa(|\vec{\ell} - \vec{\ell}'|) [\delta^2(\vec{\ell}'' + \vec{\ell}''') + \delta^2(\vec{\ell}'' - \vec{\ell}' - \vec{\ell}''')], \quad (\text{D6})$$

so, choosing  $\phi_\ell = 0$  leads to

$$C^B(\ell) = (1+q)^2 \int \frac{d^2\ell'}{(2\pi)^2} \sin(2\phi_{\ell'}) C^\kappa(\ell') C^\kappa(|\vec{\ell} - \vec{\ell}'|) \left[ \sin(2\phi_{\ell'}) + \sin(2\phi_{\vec{\ell}' - \vec{\ell}}) \right]. \quad (\text{D7})$$

Apart from geometric factors, this is of order  $\ell^2 C^\kappa(\ell) \sim 10^{-4}$  smaller than the E-mode spectrum, in qualitative agreement with the terms analyzed in [24]. Note that here the trispectrum terms may contribute an even larger correction on small scales. We leave this calculation for future work.

- 
- [1] H. Hoekstra et al., *Astrophys. J.* **647**, 116 (2006), astro-ph/0511089.
  - [2] R. Massey et al. (2007), astro-ph/0701480.
  - [3] J. Benjamin et al. (2007), astro-ph/0703570.
  - [4] A. J. Albrecht et al. (2006), astro-ph/0609591.
  - [5] A. J. Albrecht et al. (2009), 0901.0721.
  - [6] W. Hu and M. Tegmark, *Astrophys. J.* **514**, L65 (1999), astro-ph/9811168.
  - [7] K. N. Abazajian and S. Dodelson, *Phys. Rev. Lett.* **91**, 041301 (2003), astro-ph/0212216.
  - [8] K. Ichiki, M. Takada, and T. Takahashi, *Phys. Rev.* **D79**, 023520 (2009), 0810.4921.
  - [9] T. D. Kitching, A. F. Heavens, L. Verde, P. Serra, and A. Melchiorri, *Phys. Rev.* **D77**, 103008 (2008), 0801.4565.
  - [10] F. Bernardeau, L. Van Waerbeke, and Y. Mellier, *Astron. Astrophys.* **322**, 1 (1997), astro-ph/9609122.
  - [11] P. Schneider, L. van Waerbeke, B. Jain, and G. Kruse (1997), astro-ph/9708143.
  - [12] S. Dodelson, C. Shapiro, and M. J. White, *Phys. Rev.* **D73**, 023009 (2006), astro-ph/0508296.
  - [13] T. Hamana, *Mon. Not. Roy. Astron. Soc.* **326**, 326 (2001), astro-ph/0104244.
  - [14] F. Schmidt, E. Rozo, S. Dodelson, L. Hui, and E. Sheldon (2009), arXiv:0904.4702.
  - [15] D. Munshi, P. Valageas, L. van Waerbeke, and A. Heavens, *Phys. Rep.* **462**, 67 (2008).
  - [16] G. M. Bernstein and M. Jarvis, *Astron. J.* **123**, 583 (2002), arXiv:astro-ph/0107431.
  - [17] F. Bernardeau, *A&A* **338**, 375 (1998), arXiv:astro-ph/9712115.
  - [18] S. Dodelson and P. Zhang, *Phys. Rev. D* **72**, 083001 (2005), arXiv:astro-ph/0501063.
  - [19] C. Shapiro, ArXiv e-prints (2008), 0812.0769.
  - [20] J. Annis (2009), private communication.
  - [21] R. E. Smith, J. A. Peacock, A. Jenkins, S. D. M. White, C. S. Frenk, F. R. Pearce, P. A. Thomas, G. Efstathiou, and H. M. P. Couchman, *MNRAS* **341**, 1311 (2003), arXiv:astro-ph/0207664.
  - [22] R. Scoccimarro and H. M. P. Couchman, *MNRAS* **325**, 1312 (2001), arXiv:astro-ph/0009427.
  - [23] The Dark Energy Survey Collaboration, ArXiv Astrophysics e-prints (2005), arXiv:astro-ph/0510346.
  - [24] A. Cooray and W. Hu, *Astrophys. J.* **574**, 19 (2002), astro-ph/0202411.
  - [25] R. Ziour and L. Hui, *Phys. Rev. D* **78**, 123517 (2008), 0809.3101.
  - [26] G. M. Bernstein, *Astrophys. J.* **695**, 652 (2009), 0808.3400.
  - [27] L. Fu, E. Semboloni, H. Hoekstra, M. Kilbinger, L. van Waerbeke, I. Tereno, Y. Mellier, C. Heymans, J. Coupon, K. Benabed, et al., *A&A* **479**, 9 (2008), 0712.0884.
  - [28] M. White, *Astroparticle Physics* **23**, 349 (2005).
  - [29] T. Hamana, M. Takada, and N. Yoshida, *MNRAS* **350**, 893 (2004), arXiv:astro-ph/0310607.
  - [30] M. Maturi, M. Meneghetti, M. Bartelmann, K. Dolag, and L. Moscardini, *A&A* **442**, 851 (2005), arXiv:astro-ph/0412604.
  - [31] W. Hu and M. White, *Astrophys. J.* **554**, 67 (2001), arXiv:astro-ph/0010352.
  - [32] L. Hui and E. Gaztañaga, *Astrophys. J.* **519**, 622 (1999), arXiv:astro-ph/9810194.
  - [33] F. Schmidt, A. Vallinotto, E. Sefusatti, and S. Dodelson, *Phys. Rev. D* **78**, 043513 (2008), 0804.0373.
  - [34] A. Cooray and W. Hu, *Astrophys. J.* **548**, 7 (2001), arXiv:astro-ph/0004151.
  - [35] A. Cooray and W. Hu, *Astrophys. J.* **554**, 56 (2001), arXiv:astro-ph/0012087.